THE ANATOMICAL RECORD 298:680–690 (2015)

On the Anatomy of the Temporomandibular Joint and the Muscles That Act Upon It: Observations on the Gray Whale, *Eschrichtius robustus*

JOSEPH J. EL ADLI[1,2]* AND THOMAS A. DEMÉRÉ[1]
[1]Department of Paleontology, San Diego Natural History Museum, San Diego, California
[2]Department of Earth and Environmental Sciences, University of Michigan, Ann Arbor, Michigan

ABSTRACT

The temporomandibular joint and its associated musculature are described in a neonate gray whale (*Eschrichtius robustus*) and serve as the basis for direct anatomical comparisons with the temporomandibular region in other clades of baleen whales (Mysticeti). Members of the right whale/bowhead whale clade (Balaenidae) are known to possess a synovial lower jaw joint, while members of the rorqual clade (Balaenopteridae) have a nonsynovial temporomandibular joint characterized by a highly flexible fibrocartilaginous pad and no joint capsule. In contrast, the gray whale possesses a modified temporomandibular joint (intermediate condition), with a vestigial joint cavity lacking a fibrous capsule, synovial membrane, and articular disk. In addition, the presence of a rudimentary fibrocartilaginous pad appears to be homologous to that seen in balaenopterid mysticetes. The intrinsic temporomandibular musculature in the gray whale was found to include a multibellied superficial masseter and a single-bellied deep masseter. The digastric and internal pterygoid muscles in *E. robustus* are enlarged relative to the condition documented in species of *Balaenoptera*. A relatively complex insertion of the temporalis muscle on the dentary is documented in the gray whale and the low, knob-like process on the gray whale dentary is determined to be homologous with the prominent coronoid process of rorquals. Comparison with the anatomy of the temporomandibular musculature in rorquals reveals an increased importance of alpha rotation of the dentary in the gray whale. This difference in muscular morphology and lines of muscle action is interpreted as representing adaptations for suction feeding. Anat Rec, 298:680–690, 2015. © 2015 Wiley Periodicals, Inc.

Key words: *Eschrichtius robustus*; gray whale; anatomy; temporomandibular; musculature

INTRODUCTION

Comparative anatomical observations, when viewed in an evolutionary context, provide a means for examining the interplay of form and function, and can help to resolve questions of homology versus analogy and adaptation versus exaptation for particular morphological features. In cases where uncertainty exists regarding

*Correspondence to: Joseph J. El Adli, Department of Paleontology, San Diego Natural History Museum, San Diego, California. Fax: 310-756-4333. E-mail: jeladli@umich.edu

Received 28 October 2013; Revised 16 March 2014; Accepted 2 September 2014.

DOI 10.1002/ar.23109

Published online 3 March 2015 in Wiley Online Library (wileyonlinelibrary.com).

© 2015 WILEY PERIODICALS, INC.

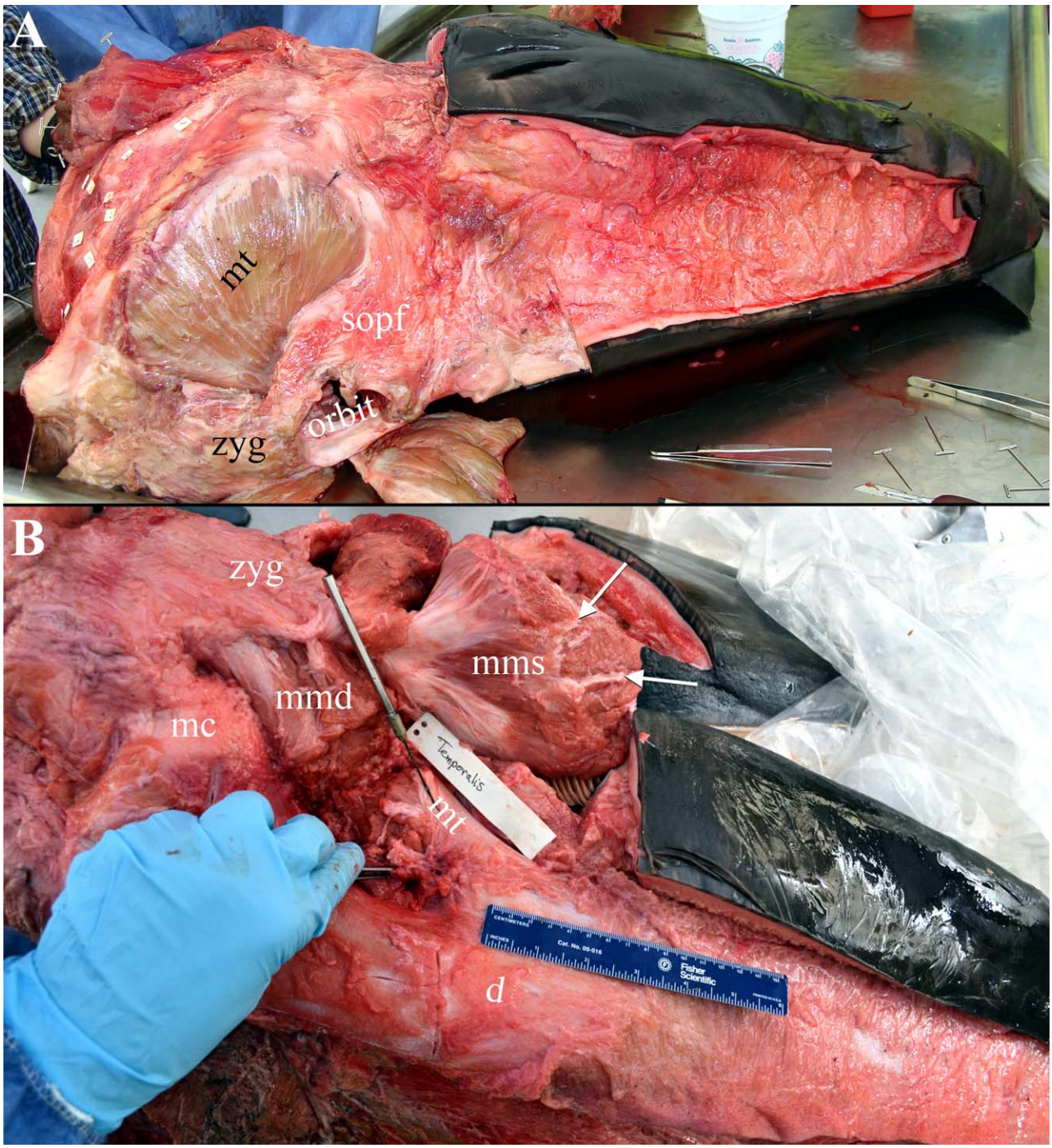

Fig. 1. *Eschrichtius robustus*, SDNHM 25307, right side of head in (**A**) dorsolateral view to show the nature of the origin of the temporalis muscle; and in (**B**) ventrolateral view to show the tendinous insertion of the temporalis muscle on the coronoid process of the dentary and the multi-bellied superficial masseter that has been cut and reflected. White arrows indicate the location of connective tissue separating the bellies of the superficial masseter. Scale bar in (B) is 15 cm in length. Abbreviations are as in Materials and Methods section.

the phylogenetic position of species and lineages, or of the taxonomic distribution of certain derived character states, basic anatomical investigations also can help better define morphological details critical to establishing relationships. Conflicts in the phylogenetic placement of certain lineages of baleen whales (Cetacea: Mysticeti) as reported in a number of recent studies (Rychel et al., 2004; Arnason et al., 2004; Deméré et al., 2005, 2008; Bisconti, 2008; McGowen et al., 2009) may serve as a case in point. Disagreement and confusion over character morphology and polarity is partly responsible for this problem, which is exacerbated by the fact that basic

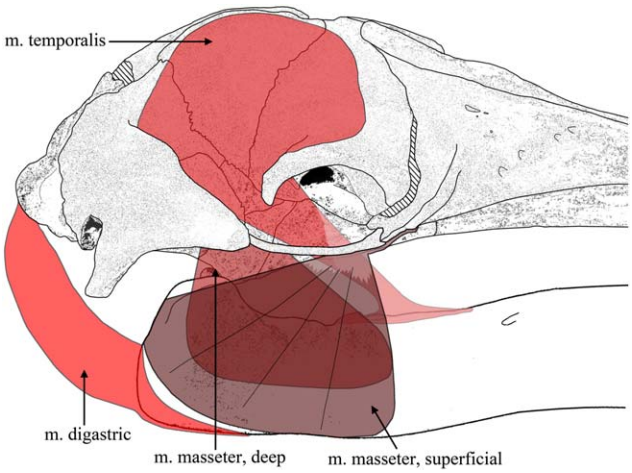

Fig. 2. *Eschrichtius robustus*, illustration of the right side of an articulated skull and dentary in lateral view with the mandibular musculature reconstructed. Illustration based on SDNHM 23516, SDNHM 23924, SDNHM 25307, and SDSU S-974.

anatomical work has not been completed for some species, especially the gray whale (*Eschrichtius robustus*) and the pygmy right whale (*Caperea marginata*). Both of these species represent the sole living members of their respective evolutionary lineages, Eschrichtiidae and Neobalaenidae. Although the biology and life history of the gray whale is certainly better known than that of the pygmy right whale, there are still major gaps in our understanding of *E. robustus*. As a purported benthic suction filter feeder (Darling et al., 1998; Dunham and Duffus, 2001; Woodward and Winn, 2006), many of the anatomical structures involved in this divergent mysticete foraging strategy have yet to be delineated. This study presents new anatomical observations on the temporomandibular joint and musculature of a neonate gray whale, makes direct comparisons with this anatomical region in rorquals, and discusses the functional role that the described features may play in gray whale suction feeding.

MATERIALS AND METHODS

Anatomical studies were conducted on the head of a 394 cm female, neonate gray whale. Details of the stranding and collection history of this specimen (SDNHM 25307) are presented in the introductory article of this Thematic Papers issue (Berta et al., 2015). Initial dissections occurred over a period of three days during April 2012 in the Department of Biology at San Diego State University and focused on anatomical structures of the right side of the skull. A second dissection session occurred over a two day period during February 2013 and focused on anatomical structures of the basicranium and left side of the skull. During the dissections individual muscles were isolated, measured, and photographed and their origins and insertions delimited. In some cases the perimeters of muscle attachment sites were scored with a scalpel into the associated bone in order to provide a physical record of the actual attachment site when the bones are eventually prepared and dried. Unfortunately, no tissue samples for histological analysis were analyzed as part of this study. The anatomical descriptions given below are based on observations made during the dissection sessions. The prepared and dry skull and dentary of a similarly aged neonate gray whale (SDSU S-974) were used during the dissection sessions to compare and correlate salient osteological features with muscle origins and insertions observed during the active dissections. Comparisons were also made with observations documented during dissection of the head of a neonate fin whale (SDSU S-970).

Measurements were taken to the nearest half centimeter with a rigid hand ruler or cloth measuring tape. Institutional abbreviations used are as follows: *LACM*, Mammalogy Department, Natural History Museum of Los Angeles County, Los Angeles, CA; *SDNHM*, Department of Birds and Mammals, San Diego Natural History Museum, San Diego, CA; *SDSU*, Department of Biology, San Diego State University, San Diego, CA. Anatomical abbreviations used in this report include: *aon*, antorbital notch; *ap*, angular process of dentary; *boc*, basioccipital; *d*, dentary; *eam*, external acoustic meatus; *hp*, hamular process of pterygoid; *j*, jugal; *lpf*, lateral palatal foramina; *max*, maxilla; *mpf*, major palatine foramen; *mc*, mandibular condyle; *md*, m. digastricus; *mg*, m. genioglossus; *mmd*, m. deep masseter; *mms*, m. superficial masseter; *mpti*, m. internal pterygoid; *mt*, m. temporalis; *npv*, nasal plate of vomer; *oc*, occipital condyle; *opc*, optic canal; *ipm*, infraorbital plate of maxilla; *pal*, palatine; *pet*, petrosal; *pgp*, postglenoid process of squamosal; *pp*, paroccipital process of exoccipital; *pte*, pterygoid; *sopf*, supraorbital process of frontal; *squ*, squamosal; *tb*, tympanic bulla; *tfo*, temporal fossa; *vom*, vomer; *zyg*, zygomatic process of squamosal.

RESULTS

Musculature

M. Temporalis. The temporalis muscle has its origin on the temporal wall and nearly fills the temporal fossa (Fig. 1A). Dorsally, the origin is demarcated by a low temporal crest, which parallels the lambdoidal crest and proceeds anteriorly onto the anterior wing of the parietal and the supraorbital process of the frontal. The temporal crest continues anteriorly until approximately the level of the anterior two-thirds of the orbit before gently curving posterolaterally toward, but never reaching, the postorbital process of the frontal. Posteriorly, the temporalis does not extend along the zygomatic crest, but instead runs along the medial face of a well-defined squamosal crease. Overall, this gives the origin of the temporalis an approximately elliptical outline in lateral view (Fig. 2).

Within the temporal fossa, the proximal portion of the temporalis is characterized by a roughly radial arrangement of muscle fibers that converge distally as the muscle wraps around and beneath the posterior margin of the supraorbital process of the frontal. Distal to the convergence of these fibers, the fleshy portion of the temporalis gives way to a strap-like, tendinous portion toward the insertion area on the dentary (Figs. 1B and 2). This tendinous portion extends anteroventrally, passing beneath the orbit and medial to the jugal and deep masseter. The bulk of the tendon attaches to the dorsal and dorsolateral surfaces of the knob-like coronoid process (Fig. 3A,B). However, two transversely

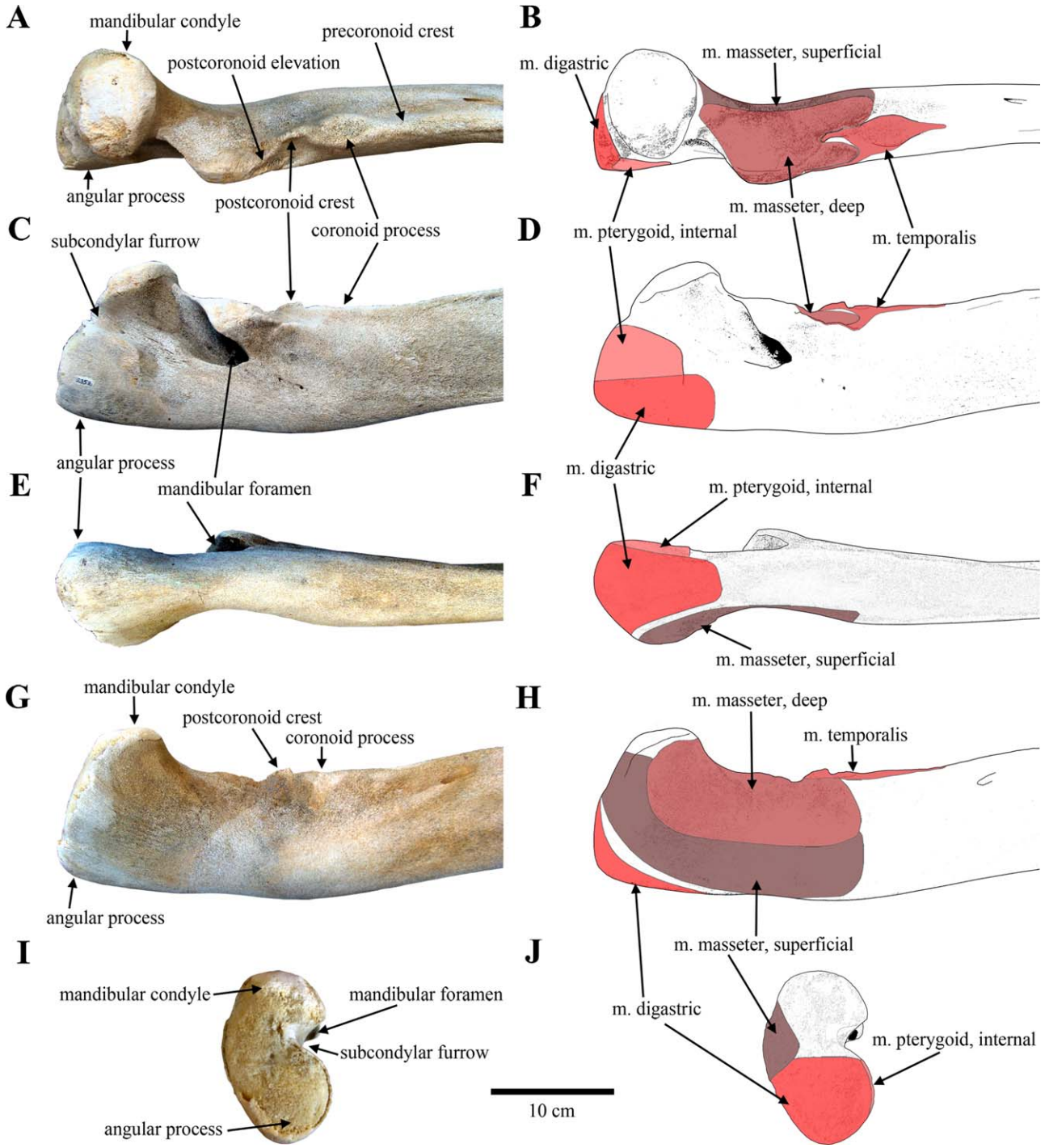

Fig. 3. *Eschrichtius robustus*, SDNHM 23516, left dentary in (**A**) dorsal; (**C**) medial; (**E**) ventral; (**G**) lateral (mirrored horizontally); and (**I**) posterior views. Illustrations of the dentary are shown with insertion areas of mandibular musculature shaded, based on dissection of SDNHM 25307, in (**B**) dorsal; (**D**) medial; (**F**) ventral; (**H**) lateral (mirrored horizontally); and (**J**) posterior views.

thin, fibrous extensions of the tendon fan out from the main tendon to insert onto the pre- and postcoronoid crests of the dentary (Fig. 3A–D). The anterior of these fibrous extensions attaches along the precoronoid crest for a distance of approximately 2 cm anterior to the coronoid process, while the posterior fibrous extension passes posteriorly along the discrete and dorsally convex post-coronoid crest for approximately 3 cm. Furthermore, a membranous, fleshy sheet of the temporalis extends posteromedially from the main tendon at the posteromedial corner of the coronoid process. This short, muscular extension passes along the medial-most

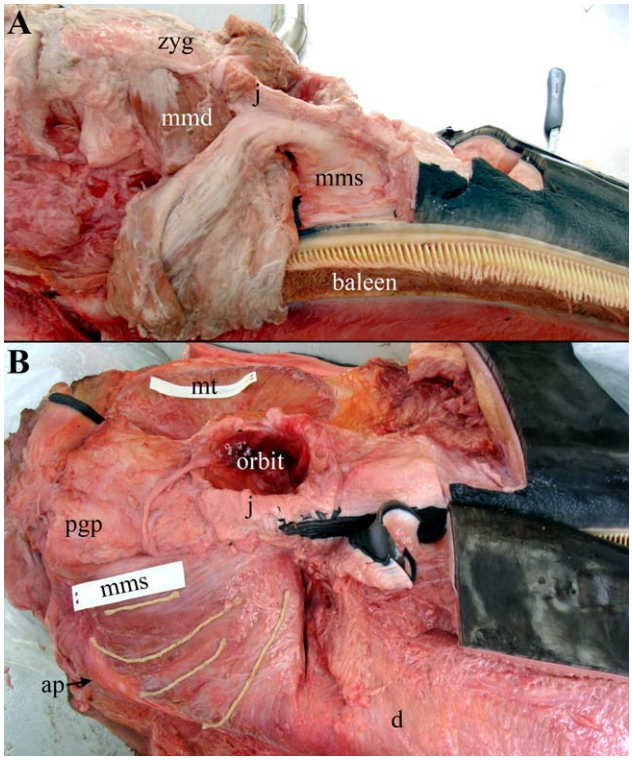

Fig. 4. *Eschrichtius robustus*, SDNHM 25307, right side of head in (**A**) ventrolateral view to show tendinous origin of the superficial masseter on the jugal and maxilla (note the cut and relaxed multiple muscle bellies of the superficial masseter); and in (**B**) lateral view to show the nature of the insertion of the superficial masseter on the dentary (strands of cord are shown in the center of each muscle belly of the superficial masseter and follow the orientation of its muscle fibers). Abbreviations are as in Materials and Methods section.

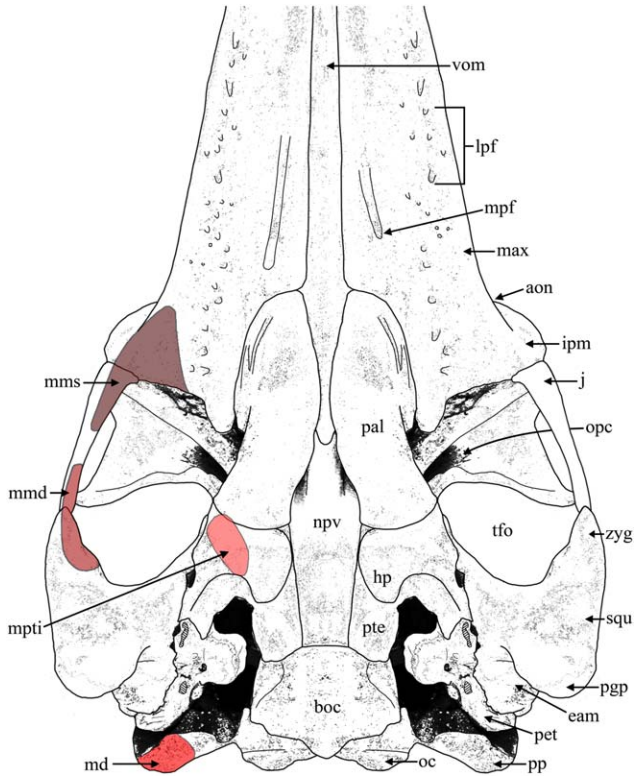

Fig. 5. *Eschrichtius robustus*, illustration of skull in ventral view based on SDNHM 23516, SDNHM 23924, SDNHM 25307, and SDSU S-974 showing the areas of origin for the mandibular musculature and osteological elements and landmarks. Abbreviations are as in Materials and Methods section.

edge of the postcoronoid elevation (Struthers, 1889; Kimura, 2002) where it laterally contacts a portion of the deep masseter (Fig. 3C,D).

M. Superficial Masseter. The masseter in *E. robustus* is differentiated into superficial and deep portions. The superficial masseter is roughly fan-shaped and exceptionally large in comparison to the condition observed in other balaenopteroids (Carté and MacAlister, 1868; Schulte, 1916; this study). The superficial masseter has a tendinous origination on the maxilla and jugal (Fig. 4A,B). Anteriorly, the tendinous origin for the superficial masseter is broader than posteriorly and covers the majority of the ventral surface of the infraorbital plate of the maxilla. In ventral view, this region of the origin is roughly deltaic in shape, with the anterior-most edge extending to approximately the level of the antorbital notch, the medial-most edge lying immediately lateral to the baleen, and the lateral-most edge extending to the posterolateral-most corner of the infraorbital plate (Fig. 5). Posterior to the infraorbital plate, the tendon proceeds posterolaterally from the posterolateral corner of the infraorbital plate along the ventromedial edge of the jugal (Figs. 2 and 5). Along the jugal, the tendon of the superficial masseter is approximately circular in cross-section as it departs from the posterior terminus of its origin beneath the orbit and descends ventrally and posteroventrally to its insertion on the dentary.

Distally, the superficial masseter becomes fleshy and fan-shaped, being divisible into at least four, radially arranged bellies (Figs. 2 and 4) each separated from one another by a sheath of connective tissue (Fig. 1B, white arrows). The fibers within each belly are generally linear and run parallel to the long axis of the belly (Figs. 1B and 4A). Their insertion is on the mediolateral and posterolateral surface of the dentary, lateral and ventral to the insertion of the deep masseter (Figs. 2 and 4B). The anterior-most belly projects ventrally from the origin and has the widest insertion area of the four bellies. Fibers within this first belly at the area of insertion are solely oriented dorsoventrally within the anterior half of the belly, but become more posteroventrally oriented within the posterior half (Fig. 4B). The two bellies immediately posterior to the anterior-most belly are discernibly narrower at their insertion area and their muscle fibers are successively more posteroventrally oriented, proceeding posteriorly. The posterior-most belly has the second largest insertion area of the four bellies and its fibers are nearly oriented horizontally from the origin. This condition of a multibellied superficial masseter has not been documented in any other species of mysticete.

The distal-most edge of the insertion area for the superficial masseter has a curvilinear length of 24 cm on the right dentary. Anteriorly, the insertion extends to

nearly reach the ventral margin of the dentary at approximately the level of the knob-like coronoid process (Figs. 2, 3H, and 4B). Posterior to this, the distal margin of the superficial masseter insertion passes on to the anterolateral corner of the angular process, but does not intrude onto the posterior or ventral surfaces of the process. The posterodorsal-most area of the insertion extends onto the posterolateral corner of the mandibular condyle and is visible in posterior view on the dentary, especially in the region of the subcondylar furrow, between the mandibular condyle and the angular process (Fig. 3I,J).

M. Deep Masseter. The deep masseter is completely covered laterally by the broader superficial masseter and was only observed after the overlying muscle was cut and reflected (Fig. 1B). In general, the deep masseter is roughly trapezoidal in shape (Fig. 2), and unlike the superficial masseter, lacks a tendinous origin. The origin for the deep masseter occurs along the posterior-most 3.5 cm of the jugal, as well as on the anterior portion of the zygomatic process (Fig. 5), to have an overall anteroposterior length, at the origin, of 7 cm. On both the jugal and the zygomatic process, the origin for the deep masseter occurs on the medial half of the ventral surface (Fig. 5). The deep masseter, however, also slightly extends as a sheet onto the medial surface of the zygomatic process.

The main body of the deep masseter projects anteroventrally (Fig. 2) to insert on both the dorsal and lateral portions of the neck of the dentary (=the portion of the dentary between the coronoid process and the mandibular condyle; Lambertsen et al., 1995), filling the dorsal half of the shallow masseteric fossa (Fig. 3H). The muscle fibers of the deep masseter are linear and run anteroventrally from the origin parallel to the long axis of the muscle. Along the ventral margin of the insertion, the muscle fibers of the deep masseter merge with those of the anterior belly of the superficial masseter in the area of their common insertion. Unlike the superficial masseter, the deep masseter is composed of a single, undifferentiated muscle.

The insertion for the deep masseter is larger in area than that of the superficial masseter and has a relatively complex interaction with the insertion for the temporalis. The anterodorsal portion of the former bifurcates to pass on either side of the postcoronoid crest and surround the posteriorly extended tendinous portion of the temporalis insertion (Fig. 3B,D). In lateral view, the distal-most portion of the deep masseter insertion occurs immediately dorsal to the insertion for the superficial masseter, and follows a similar, but dorsally placed, curvilinear path (Figs. 2 and 3H). Unlike the superficial masseter, however, the deep masseter does not reach the level of the mandibular condyle. From its anteroventral corner, the anterior edge of the insertion area for the deep masseter extends posterodorsally along the anterior portion of the neck of the dentary, toward the posterior edge of the knob-like coronoid process. The deep masseter then follows the lateral edge of the coronoid process and the postcoronoid crest (Fig. 3B,H). An anterior slip of the deep masseter passes along the medial margin of the postcoronoid crest to occupy the small, medial fossa formed by this crest.

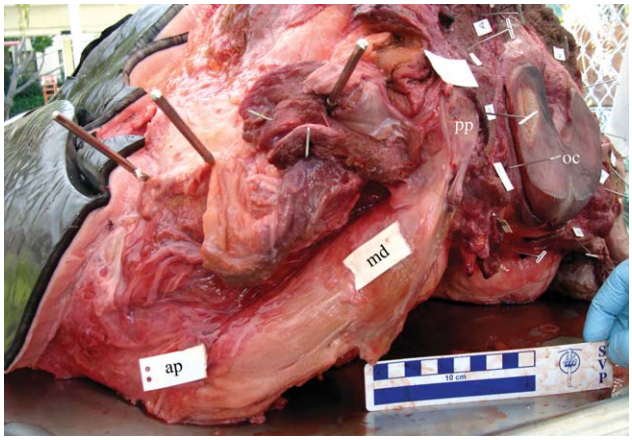

Fig. 6. *Eschrichtius robustus*, SDNHM 25307, posterolateral view of left side of head showing the digastric muscle and its area of origin and insertion. Scale bar is 10 cm in length. Abbreviations are as in Materials and Methods section.

M. Digastric. The digastric muscle is a single muscle with no evidence of a division into two bellies. Overall, the digastric is rope-like, with a roughly circular to elliptical origin on the ventral most corner of the paroccipital process of the exoccipital measuring 3.5 cm anteroposteriorly and 3 cm mediolaterally (Figs. 5 and 6). The digastric is attached to the exoccipital by a short tendon, which rapidly gives way to a cylindrical, fleshy belly that expands in thickness to measure 6.5 cm in diameter at its broadest point, near the midpoint of the muscle (Fig. 6). Distal to the origin, the digastric runs anteroventrally toward the angular process of the dentary and ventral to the postglenoid process (Fig. 2). The muscle fibers of the digastric follow the length of the curved longitudinal axis of the muscle from origin to insertion (Fig. 6). The digastric inserts onto the angular process of the dentary with no tendinous portion being visible near the bone surface. The insertion covers the entire posterior and ventral surfaces of the angular process (Fig. 3F,J). Laterally, the insertion occupies only a small portion of the posteroventral corner of the angular process and is separated from contact with the superficial masseter by a narrow region of bone lacking any attached musculature (Fig. 3H). On the medial side, the digastric insertion extends well onto the medial surface of the angular process to a contact with the insertion of the more dorsally placed internal pterygoid muscle (Fig. 3D). The anterior-most edge of the digastric contacts and partially covers a sheet of periosteum, which in turn forms the medial wall of a canal for passage of the lingual nerve. Ventrally, the digastric inserts over nearly the entire ventral surface of the angular process of the dentary (Fig. 3F).

M. Internal Pterygoid. The pterygoid muscle could not be differentiated into distinct external and internal bodies (=lateral and medial pterygoid, respectively). Instead, a single internal pterygoid muscle was observed (Fig. 7) to originate from the ventrolateral portion of the pterygoid bone, lateral to the main body of the hamular process and just posterior to the posterolateral corner of the pterygoid-palatine suture on the palate

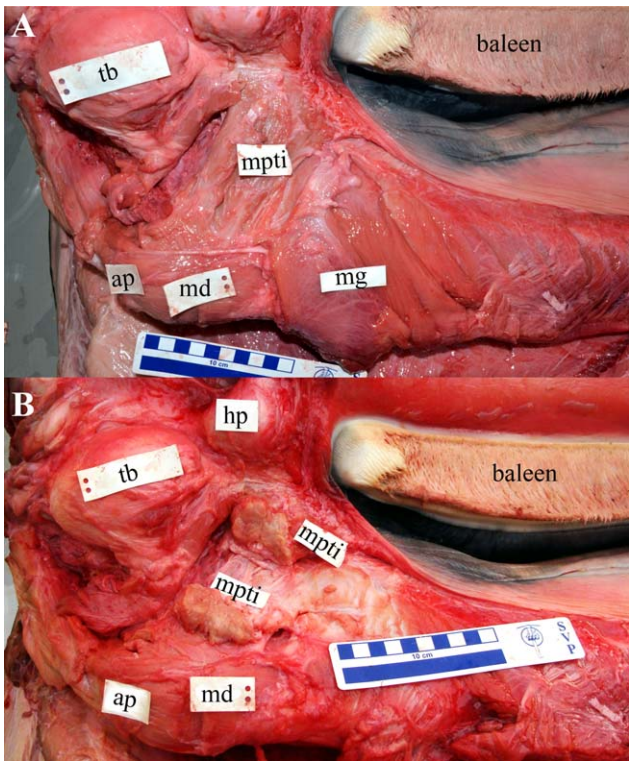

Fig. 7. *Eschrichtius robustus*, SDNHM 25307, ventral view of right side of head showing the internal pterygoid muscle in (**A**) external view; and in (**B**) cross-section. Scale bar is 10 cm in length. Abbreviations are as in Materials and Methods section.

(Fig. 5). The origin, however, did not extend medially onto the ventral surface of the hamular process, and, in fact, the hamular process was not covered by any muscle tissue. The origin on the pterygoid is roughly rhomboid in shape, and measures approximately 6 cm long (anterolaterally to posteromedially) and 3 cm wide (normal to the long axis). In ventral view, the internal pterygoid muscle is strap-like and slightly narrows in width toward the area of insertion. The muscle runs posterolaterally from the origin on the pterygoid bone to insert on the medial surface of the angular process of the dentary, with muscle fibers running linearly along the longitudinal axis (Fig. 7). The insertion for the internal pterygoid is located on the dorsal half of the angular process and is hemispherical in general outline (Fig. 3D). Ventrally, the margin for the insertion of the internal pterygoid is linear and runs approximately anteroposteriorly along a contact with the more ventrally placed digastric (Fig. 3F). Dorsal to this, the dorsal margin of the internal pterygoid insertion follows the medial margin of the slightly medially protruding angular process, just ventral to the subcondylar furrow (Fig. 3C,D). The internal pterygoid does not extend onto the posterior edge of the angular process, which is instead entirely covered by the digastric (Fig. 3J). Likewise, the internal pterygoid does not extend into the subcondylar furrow, which instead is occupied by the inferior alveolar artery just distal to its branching from the mandibular portion of the maxillary artery.

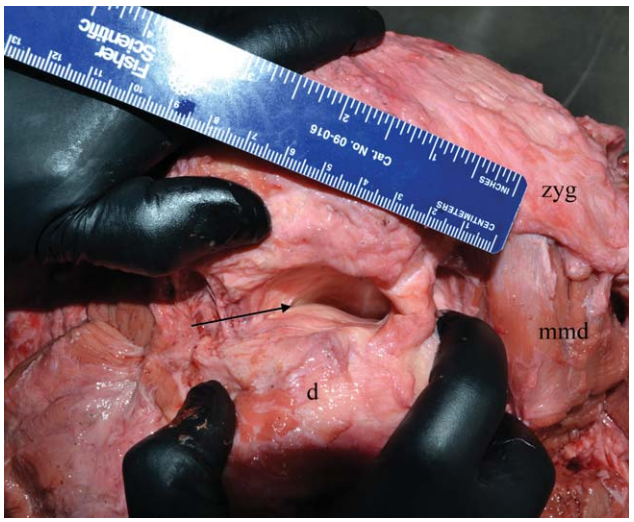

Fig. 8. *Eschrichtius robustus*, SDNHM 25307, lateral view of right side of temporomandibular joint showing size and location of modified joint cavity (posterior edge of cavity marked by black arrow). Abbreviations are as in Materials and Methods section.

Temporomandibular Joint

Prior to dissection of the temporomandibular joint the posterodorsal surface of the mandibular condyle was observed to lie approximately 3.5 cm from the anterior face of the postglenoid process of the squamosal. This measurement was made while the joint was in a relaxed position. The temporomandibular joint was spanned laterally by a ligament, which was 7 cm in length anteroposteriorly and extended from the anterolateral side of the postglenoid process to the posterior and posterodorsal margin of the mandibular condyle. Physical manipulation of the dentary suggests that this ligament restricts anterior and mediolateral displacement of the condyle (omega rotation of Lambertsen et al., 1995), but does not impede depression of the mandible (delta rotation of Lambertsen et al., 1995) or rotation about the long axis of the dentary (alpha rotation of Lambertsen et al., 1995).

Deep to the temporomandibular ligament, the temporomandibular joint was observed to consist of an approximately 2 cm thick mass of white tissue, similar in texture and density (but not volume) to the fibrocartilaginous pad reported in the temporomandibular joint of balaenopterids (Lambertsen et al., 1995). Although, no histological analysis of this tissue was conducted, it is here considered to be fibrocartilage based on presumed homology with the balaenopterid fibrocartilage pad. Once the surrounding ligament was removed, the mass of dense, white tissue was found, upon manipulation, to be highly elastic and compressible. This "fibrocartilage pad" attached to the entire anterior surface of the postglenoid process and extended medially to fill a portion of the adjacent tympanosquamosal recess. The "fibrocartilage pad", however, did not extend across the tympanosquamosal recess and was not present on the lateral side of the postglenoid process.

Further dissection of the temporomandibular joint revealed a single, small, but discrete joint cavity positioned between the circular, posterodorsally oriented

surface of the mandibular condyle and the anteroventrally concave glenoid fossa of the squamosal (Fig. 8). This joint cavity was approximately elliptical in shape and measured 5.2 cm anteroposteriorly and 4.4 cm transversely. The cavity was smaller in diameter than, and roughly centered on, the middle of the mandibular condyle and did not extend laterally and medially to encapsulate the entire "articular" surfaces of the condyle or glenoid fossa. In addition, the "articular" surface of the mandibular condyle was not covered with fibrous articular tissue and there was no obvious synovial membrane, fibrous capsule, or articular disk. However, the "articular" surface of the mandibular condyle did have a layer of white, pliable tissue marked peripherally by a ring of white, denser tissues. Unfortunately, the composition of this tissue was not determined. A small volume (<0.1 mL) of viscous fluid was observed within the joint cavity, but attempts to extract a pure sample of this fluid were unsuccessful. Thus, it could not be determined whether this was actual synovial fluid. The "fibrocartilage pad" filled the portion of the temporomandibular joint between the postglenoid process and the small joint cavity and extended both laterally and medially around the mandibular condyle.

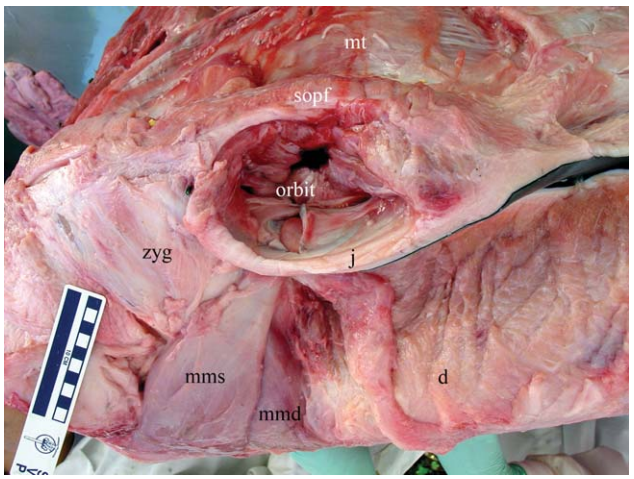

Fig. 9. *Balaenoptera physalus*, SDSU S-970, lateral view of right side of head showing the nature of the superficial and deep masseters. Scale bar is 10 cm in length. Abbreviations are as in Materials and Methods section.

DISCUSSION

The anatomy of the gray whale temporomandibular joint and the muscles that act upon it, as described above, provides an opportunity to make direct comparisons with the temporomandibular region in other balaenopteroid (rorquals + gray whales) lineages. Furthermore, these observations, coupled with an understanding of the general phylogenetic relationships among mysticete lineages, allow for investigation of possible evolutionary trends within the history of balaenopteroid mysticetes. Finally, the morphology of the temporomandibular region presents an opportunity to look for possible correlations between form and function as relates to the biomechanics of suction feeding in gray whales.

Comparison of the temporomandibular musculature in the neonate *E. robustus* with that documented in rorquals (Carté and MacAlister, 1868; Schulte, 1916; personal observations) reveals interesting differences and similarities. Most notably, the gray whale superficial masseter is relatively larger in its overall size, as well as the size and extent of its areas of origin and insertion. In a neonate fin whale (*Balaenoptera physalus*) dissected at SDSU (SDSU S-970), the superficial masseter was a single, relatively strap-like muscle that was minimally expanded distally with a relatively small, muscular origin and insertion (Fig. 9). The origin of the superficial masseter in *B. borealis* and *B. acutorostrata* was not documented by Schulte (1916) or Carté and MacAlister (1868), but was reported by Lambertsen and Hintz (2004) to extend onto the ventral surface of the infraorbital plate of the maxilla in the several rorquals species that they studied. In *B. physalus* (SDSU S-970) the strap-like muscle extended posteroventrally from the jugal to an elliptical insertion on the ventrolateral portion of the angular process of the dentary. Both *B. borealis* and *B. physalus* have been reported to possess a single bellied superficial masseter that runs posteroventrally from the posterior portion of the jugal to insert via an elliptical attachment on the posterolateral surface of the dentary (Schulte, 1916). This condition contrasts markedly with the condition in *E. robustus*, where the more massive insertion of the multi-bellied superficial masseter nearly covers the entire lateral surface of the mandibular condyle, angular process, and ventral half of the neck of the dentary (Figs. 2 and 3). Based on the apparent line of action of the superficial masseter in rorquals, contraction of the muscle likely results in several related movements of the dentary including elevation of the dentary (delta rotation), pulling the dentary anteriorly, and, in concert with the pterygoid muscle, rotating the mandible about its longitudinal axis (alpha rotation). Although the superficial masseter in *E. robustus* is likely capable of similar actions of mandibular elevation, protraction, and longitudinal rotation, the multiple bellies that fan out ventrally to insert along nearly the entire posterolateral portion of the dentary grossly resemble the deltoid muscle, and, like the deltoid, suggest a greater force production but smaller range of motion for the superficial masseter. Thus, as configured, the gray whale superficial masseter allows for increased power in controlling the lower jaw during alpha rotation, while also limiting the degree of delta rotation (angle of gape) of the lower jaw. Furthermore, the presence of multiple bellies within the superficial masseter suggests increased fine motor control during alpha rotation, as has been documented in other multibellied muscles (Brown et al., 2007). This is important, given that alpha rotation appears to be a critical component of gray whale suction feeding, wherein the dentaries alternately rotate laterally and medially to occlude the lower lips against the upper jaws during mediolateral pumping of water into and out of the oral cavity (Johnston et al., 2010). In rorquals outward alpha rotation of the lower jaw increases oral surface area and appears to be largely accomplished by relaxation of the temporalis to break the oral seal between the upper and lower lips (Lambertsen et al., 1995). Inward alpha rotation is more complex in rorquals and accomplished by both muscular and mechanical components of the

temporomandibular region, but at the end of an engulfment event primarily involves contraction of the temporalis to reseal the oral cavity (Goldbogen et al., 2011).

The deep masseter in *B. physalus* (SDSU S-970) was found to be roughly rectangular in shape and from its origin on the anteroventral portion of the zygomatic process of the squamosal was directed ventrally to insert along a relatively narrow band that extended vertically from the dorsal margin of the mandibular neck across the masseteric fossa nearly to the ventral margin of the dentary (Fig. 9). In this configuration the insertion areas for the superficial and deep masseter muscles are separated on the lateral surface of the dentary. The insertion for the deep masseter in *B. borealis*, as reported by Schulte (1916), appears to be larger than observed in the *B. physalus* neonate and fills the majority of the masseteric fossa on the neck of the dentary. This apparent difference between *B. physalus* and *B. borealis* may or may not be real and should be investigated with additional dissections. Schulte (1916) also indicated that the insertion for the deep masseter in *B. borealis* was located anterior or anterodorsal to the insertion of the superficial masseter, as here confirmed in *B. physalus* (SDSU S-970). In both species of *Balaenoptera*, neither insertion of the masseter muscles extends onto the lateral surface of the mandibular condyle. Although the origin of the deep masseter in *E. robustus* was similar to that observed in *B. physalus*, the distal body of the muscle was more anteroposteriorly expanded, with an area of insertion that extended from the level of the coronoid process, posteriorly across the entire masseteric fossa to cover much of the lateral surface of the mandibular condyle. The line of action for the deep masseter in balaenopterids is therefore directed slightly anteroventrally from the zygomatic process, suggesting that contraction of this muscle acts to both elevate the mandible and retract it posteriorly. However, in *E. robustus* the line of action appears to be more ventrally directed than that observed in rorquals, which implies a greater importance for the muscle in alpha rotation over posterior movement of the dentary, as well as elevation of the dentary. Furthermore, the presence of a strap-like temporomandibular ligament between the squamosal and mandibular condyle in *E. robustus* likely reduces the need to pull the mandible posteriorly in gray whales, unlike the more loosely articulated temporomandibular joint of balaenopterids.

The temporalis muscle is similar in both balaenopterids and *E. robustus* and occurs as a convergent muscle that essentially fills the entire temporal fossa from its origin along the temporal crest of the braincase (Carté and MacAlister, 1868; Schulte, 1916; Lambertsen et al. 1995). The grossly radially arranged muscle fibers converge ventrally in the temporal fossa where they pass posteroventrally around the posterior margin of the supraorbital process of the frontal. In *B. physalus* (SDSU S-970) and other balaenopterids (Schulte, 1916; Lambertsen et al., 1995) the temporalis terminates in a roughly cylindrical tendinous insertion that surrounds and entirely invests the finger-like and laterally deflected coronoid process of the dentary. The temporalis insertion is grossly similar in *E. robustus* in that the muscle fibers distally converge to form a tendinous insertion on the low, knob-like coronoid process. Anatomical details of that insertion, however, are somewhat unique in *E. robustus* in having several complex tendinous and fleshy components, which attach along the ridge-like precoronoid and postcoronoid crests, as well as along the medial edge of the postcoronoid elevation. Andrews (1914) characterized the dentaries of *E. robustus* as "...without coronoid processes these being represented only by flattened tubercles." However, the main tendinous insertion of the temporalis clearly demonstrates that the low, knob-like process on the dorsal edge of the dentary is homologous to the finger-like coronoid process in balaenopterids. The morphological complexity of the coronoid region in *E. robustus* is illustrated in Fig. 3A,C, and consists of the expanded knob-like coronoid process with precoronoid and postcoronoid crests, the latter with an adjacent medially placed postcoronoid elevation. The primary action of the temporalis in both *E. robustus* and species of *Balaenoptera* is to elevate the dentary (delta rotation). However, the elongation and lateral deflection of the coronoid process in balaenopterids has been proposed as an adaptation for inward rotation of the dentary (alpha rotation) to seal the oral cavity (Lambertsen et al., 1995). The reduction in size of the coronoid process in *E. robustus* suggests that the primary action of the temporalis in this mysticete lineage is for delta rotation and not alpha rotation of the dentary.

The digastric muscle has not been well documented in mysticetes and, unfortunately, was not observed in the dissection of the neonate fin whale (SDSU S-970) due to the way the head was separated from the torso during processing of the stranded animal. Schulte (1916) described the digastric (=depressor mandibulae of Schulte, 1916) as having two bellies and illustrated the origin of the digastric as occurring on the posterior surface of the postglenoid process of the squamosal (Schulte, 1916: Plate LV). Furthermore, that author observed the digastric to have an insertion area along all surfaces of the angular process of the dentary, with an especially close contact with the superficial masseter laterally. Unlike the condition reported by Schulte (1916) in *B. borealis*, the digastric of *E. robustus* consisted of only a single, rope-like muscle that originated on the ventral surface of the paroccipital process of the exoccipital. The insertion on the angular process of the dentary was clearly differentiated, medially and ventrally, but had only a limited insertion on the lateral surface of the angular process and was widely separated from the superficial masseter. It is unclear whether the two bellies of the digastric and positioning of the origin of the muscle on the postglenoid process reported by Schulte (1916) represent observational errors. However, it seems unlikely that these two closely related taxa would have such differently constructed digastric muscles. In most odontocetes, as well as pigs and goats, the digastric has been described as having a single-bellied condition (Lawrence and Schevill, 1965; Getty, 1975; Werth, 1992; Reidenberg and Laitman, 1994). This single-bellied condition previously has not been documented in mysticetes. The action of the digastric is to abduct the lower jaw. However, muscular abduction of the lower jaw may be more important in gray whales than in rorquals since the latter can rely on forward momentum of the body and relaxation of the oral seal to initiate jaw abduction during lunge feeding (Lambertsen et al., 1995; Goldbogen et al., 2011).

The temporomandibular joint of a yearling specimen (LACM 95548) of *E. robustus* was investigated by Johnston et al. (2010), who described the joint as being nonsynovial, the condition documented in species of balaenopterid mysticetes (Hunter, 1787; Carté and MacAlister, 1868; Schulte, 1916; Lambertsen et al., 1995). The discovery of a discrete, albeit modified, joint cavity in the temporomandibular joint of a neonate gray whale (SDNHM 25307; this study) contradicts the findings of Johnston et al. (2010). An important factor to consider in this apparent conflict is the fact that the yearling specimen (LACM 95548) was dissected in an advanced stage of decomposition, which may have made it difficult to accurately determine the true soft anatomy of this feature. It is also possible that the different findings could be the result of ontogenetic changes, wherein a modified joint cavity present in neonates is eventually lost with increasing age. In any event, it is noteworthy that the temporomandibular joint observed in SDNHM 25307 possesses some, but not all, of the characteristic features of a true synovial joint. Although there is a joint cavity, the cavity is relatively small and does not encapsulate the mandibular condyle. In addition, there is no fibrous articular tissue covering the articular surface of the mandibular condyle, no obvious synovial membrane, no fibrous capsule, and no articular disk. As thus described, this modified temporomandibular joint configuration has not been observed in any other mysticete, nor has it been documented in any other mammals. In the context of a morphological series that consists of balaenids, with their synovial temporomandibular joint (the pleisiomorphic condition), at one end and rorquals, with their non-synovial jaw joint (the apomorphic condition), at the other end, the modified jaw joint of gray whales can be viewed as a separate, intermediate condition. In this context the gray whale's temporomandibular joint, with its modified joint cavity, may represent a vestigial synovial joint.

CONCLUSIONS

The differences in mandibular musculature noted between species of *Balaenoptera* and *Eschrichtius* may be viewed as adaptations for the divergent feeding strategy of the gray whale. Observations of feeding gray whales have revealed a greatly decreased ability to achieve large gape angles (relative to rorquals), while at the same time exhibiting an increased reliance on the rotation of the dentary along its long axis in order to create fluid flow and to physically move prey-laden sediment into the oral cavity. This action of alpha rotation requires modification of the mandibular musculature that controls lateral and medial movement of the dentary about its long axis. These modifications are evident in the enlarged masseters with more vertically oriented lines of muscle action relative to the condition observed in species of *Balaenoptera*. Furthermore, the multiple bellies of the superficial masseter in *E. robustus* suggest greater precision and selective calibration in the directionality of movement of each dentary. Finally, the enlargement of the mandibular muscles likely aids the gray whale in depressing and elevating the dentary under the increased load of sediment in the oral cavity during feeding.

ACKNOWLEDGEMENTS

The authors would like to thank Moss Landing Marine Laboratories for collecting and providing SDNHM 25307 for dissection during this study. K. Albertine, W. Ary, A. Berta, M.A. Chocas, T. Cranford, E. Ekdale, S. Kienle, J. Martin, J. Reidenberg, D. Silva, M. Smallcomb, L. Witmer, and N. Zellmer are thanked for their participation and help during the dissection. This study benefited from discussions with A. Berta, E. Ekdale, J. Reidenberg, A. Reizian, and L. Witmer, for which we thank them. The careful evaluation of the original manuscript by two anonymous reviewers resulted in the overall improvement in this contribution.

LITERATURE CITED

Andrews RC. 1914. The California Gray Whale (*Rhachianectes glaucus* Cope): its history, habits, external anatomy, osteology and relationship. Monographs of the Pacific Cetacea. Mem Amer Mus Nat Hist 1:227–287.

Arnason U, Gullberg A, Janke A. 2004. Mitogenomic analyses provide new insights into cetacean origin and evolution. Gene 333:27–34.

Berta A, Ekdale EG, Deméré TA, Reidenberg JS. 2015. Introduction to the anatomy of the head of a neonate gray whale (Mysticeti, *Eschrichtius robustus*). Anat Rec 298:643–647.

Bisconti M. 2008. Morphology and phylogenetic relationships of a new eschrichtiid genus (Cetacea: Mysticeti) from the Early Pliocene of northern Italy. Zool J Linn Soc 153:161–186.

Brown JMM, Wickham JB, McAndrew DJ, Huang XF. 2007. Muscles within muscles: coordination of 19 muscle segments within three shoulder muscles during isometric motor tasks. J Electromyogr Kinesiol 17:57–73.

Carté A, MacAlister A. 1868. On the anatomy of *Balaenoptera rostrata*. Philos Trans R Soc Lond 158:201–261.

Darling JD, Keogh KE, Steeves TE. 1998. Gray whale (*Eschrichtius robustus*) habitat utilizations and prey species off Vancouver Island, B. C. Mar Mam Sci 14:692–720.

Deméré TA, Berta A, McGowen MR. 2005. The taxonomic and evolutionary history of fossil and modern balaenopteroid mysticetes. J Mam Evol 12:99–143.

Deméré TA, McGowen MR, Berta A, Gatesy J. 2008. Morphological and molecular evidence for a stepwise evolutionary transition from teeth to baleen in mysticete whales. Syst Biol 57:15–37.

Dunham JS, Duffus DA. 2001. Foraging patterns of gray whales in central Calyoquot Sound, British Columbia, Canada. Mar Ecol Prog Ser 223:299–310.

Getty R. 1975. Sisson and Grossman's the anatomy of the domestic animals. Vols. 1 and 2. 5th ed. Philadelphia: W.B. Saunders Co.

Goldbogen J, Calambokidis J, Oleson E, Potvin J, Pyenson ND, Schorr G, Shadwick R. 2011. Mechanics, hydrodynamics and energetics of blue whale lunge feeding: efficiency dependence on krill density. J Exp Biol 214:131–146.

Hunter J. 1787. Observations on the structure and oeconomy of whales. Philos Trans R Soc Lond 77:307–352.

Johnston C, Deméré TA, Berta A, Yonas J, St Leger J. 2010. Observations on the musculoskeletal anatomy of the head of a neonate gray whale (*Eschrichtius robustus*). Mar Mam Sci 26:186–194.

Kimura T. 2002. Feeding strategy of an early Miocene cetothere from the Toyama and Akeyo Formations, central Japan. Paleontol Res 6:179–189.

Lambertsen R, Hintz RJ. 2004. Maxillomandibular cam articulation discovered in North Atlantic minke whale. J Mammal 85:446–452.

Lambertsen R, Ulrich N, Straley J. 1995. Frontomandibular stay of Balaenopteridae: a mechanism for momentum recapture during feeding. J Mammal 76:877–899.

Lawrence B, Schevill WE. 1965. Gular musculature in delphinids. Bull Mus Comp Zool 133:1–65.

McGowen MR, Spaulding M, Gatesy J. 2009. Divergence date estimation and a comprehensive molecular tree of extant cetaceans. Mol Phylogenet Evol 53:891–906.

Reidenberg JS, Laitman JT. 1994. Anatomy of the hyoid apparatus in odontoceti (toothed whales): specializations of their skeleton and musculature compared with those of terrestrial mammals. Anat Rec 240:598–624.

Rychel AL, Reeder TW, Berta A. 2004. Phylogeny of mysticete whales based on mitochondrial and nuclear data. Mol Phylogenet Evol 32:892–901.

Schulte W. 1916. Anatomy of a foetus of *Balaenoptera borealis*. Mem Amer Mus Nat Hist 1.

Struthers J. 1889. On some points in the anatomy of a *Megaptera longimana*. Part IV. J Anat Physiol 23:308–335, 358–373.

Werth AJ. 1992. Anatomy and evolution of odontocete suction feeding. PhD thesis. Cambridge: Harvard University Press.

Woodward BL, Winn JP. 2006. Apparent lateralized behavior in gray whales feeding off the central British Columbia coast. Mar Mam Sci 22:64–73.